

Coalescence of nanometer silver islands on oxides grown by filtered cathodic arc deposition

Eungsun Byon,^{a)} Thomas W. H. Oates,^{b)} and André Anders^{c)}

Lawrence Berkeley National Laboratory, University of California, 1 Cyclotron Road, Berkeley, California 94720-8223

(Received 27 August 2002; accepted 15 January 2003)

Ultrathin silver films have been deposited on glass and oxide-coated glass using filtered cathodic arc deposition and, for comparison, magnetron sputtering. The energetic differences between these deposition methods lead to initially different film properties. Silver films made by cathodic arc deposition show an earlier onset of island coalescence, indicating a lower aspect ratio than islands produced by evaporation and sputtering. However, the as-deposited films are thermodynamically unstable, exhibiting changes on a timescale of minutes. While films of islands tend to increase their sheet resistance with time, the sheet resistance of contiguous films shows a decrease. Both effects can be explained by silver mobility driven to minimize film and interfacial energy. © 2003 American Institute of Physics. [DOI: 10.1063/1.1558955]

Spectrally selective, transparent coatings are of great interest for energy-efficient window coatings. In cold climates, low-emittance (low-E) coatings with high solar transmittance ($0.3 < \lambda < 3 \mu\text{m}$) and high thermal infrared (IR) reflectance ($3 < \lambda < 100 \mu\text{m}$) are required, while in warm climates solar control coatings of high luminous transmittance ($0.4 < \lambda < 0.7 \mu\text{m}$) and high near-infrared reflectance ($0.7 < \lambda < 3 \mu\text{m}$) are beneficial. Both types of coatings can be obtained by embedding a thin metal film between antireflecting dielectric layers.¹ Low emittance and high infrared reflectivity are directly related to the sheet resistance of the metal layer.² Silver is the metal of choice because of its high conductivity and color-neutral transmission in the visible range of the spectrum. To maximize transmission in the visible and reflectance in the IR, it is desirable to produce a very thin silver film that is as conducting as possible.

Silver on oxides grows in the Volmer–Weber mode, i.e., silver islands are formed before a continuous film is obtained. Ultrathin silver films consisting of islands show relatively high absorption in the visible and low IR reflection. Coalescence of silver islands is therefore crucial for obtaining the desired optical properties. Silver films of about 12 nm thickness are produced for low-E application on a very large scale by magnetron sputtering on oxide-coated flat glass.² While nucleation, island growth, and coalescence has been investigated for evaporated³ and sputtered⁴ silver films, little is known about silver films synthesized by energetic condensation. In energetic condensation, film-forming atoms or ions arrive at the substrate surface with hyperthermal energies, typically in the range of 10–100 eV, leading to subplantation and nanoscale thermal spikes around the arriving particle's impact location.⁵ Filtered cathodic arc vacuum (FCVA) deposition is a prominent example for energetic condensation.

Thin gold films deposited by FCVA deposition have a lower roughness than evaporated and sputtered films.⁶ In this work we focus on coalescence of silver on oxide surfaces produced by FCVA deposition.

The experimental setup is shown in Fig. 1. A miniature pulsed cathodic arc plasma source⁷ with a cylindrical silver cathode of 6.25 mm diameter was operated with a 10-stage pulse-forming network. The arc current pulses had a rectangular shape with 1.2 kA amplitude and 620 μs pulse width, with a pulse repetition rate of 1.6 pps. The plasma source injected streaming silver plasma into a 90° magnetic macro-particle filter,⁸ which was used to remove macroparticles produced at cathode spots. Neutral silver vapor, if present in the flow, is also removed by the filter, and thus fully ionized silver plasma arrived at the substrates, which were located 200 mm from the filter exit. The silver plasma streaming velocity was 11 100 m/s, corresponding to an average kinetic energy of 70 eV, and the mean ion charge state was 2.1 (Ref. 9). The chamber was cryogenically pumped to a base pressure of about 10^{-4} Pa; no process gas was needed or used.

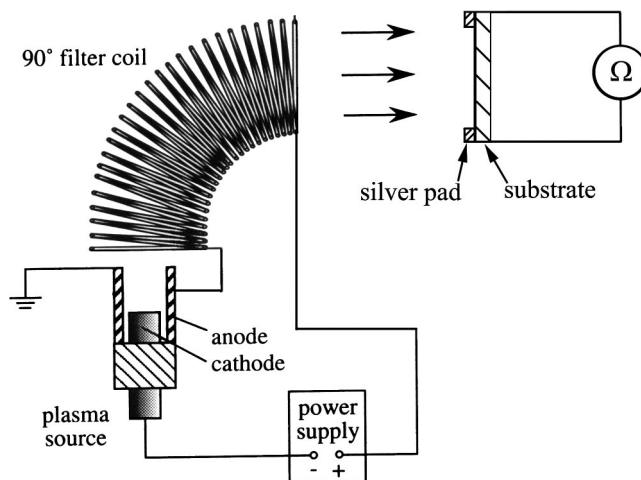


FIG. 1. Experimental setup for filtered cathodic vacuum arc (FCVA) deposition of thin metal films.

^{a)}Current address: Surface Engineering Department, Korean Institute of Machinery and Materials, 16 Sangnam-Dong, Changwon 641-010, Korea.

^{b)}Current address: Applied and Plasma Physics, School of Physics, University of Sydney, 2006, Australia.

^{c)}Author to whom correspondence should be addressed; electronic mail: aanders@lbl.gov

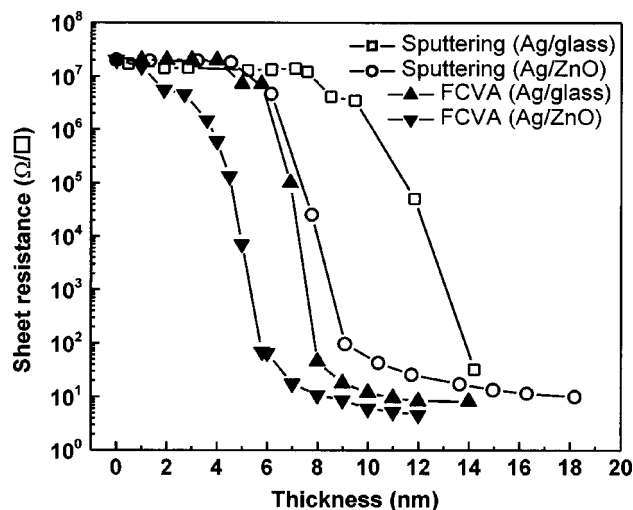


FIG. 2. Sheet resistance of sputtered and filtered arc deposited silver films as a function of incident silver dose, which is expressed as nominal film thickness, measured immediately after completion of deposition.

Uncoated glass standard microscope slides, magnetron-sputtered zinc-oxide-coated glass, and titanium-oxide-coated glass were used as substrates. The samples were mounted on a water-cooled substrate holder. The substrate temperature was generally near room temperature although the surface is subject to heating by the deposition process. It is known¹⁰ that the TiO₂ layer is amorphous while the ZnO layer is polycrystalline with {0001} orientation.

Coalescence of silver islands can be detected by measuring the onset of electronic conduction. The film resistance was measured *in situ* during deposition. Two silver contact pads, $\sim 1 \mu\text{m}$ thick, were deposited on the 25 mm wide samples prior to the experiments. The contact pads were 25 mm apart and thus an area of 25 mm \times 25 mm was defined. The resistance between the contact pads was measured using a Keithley 177 precision multimeter, directly giving the sheet resistance in ohms per square. A possible effect of the measuring current was considered as will be discussed.

The deposition rate was calibrated *ex situ* by measuring step heights of a relatively thick film (100 nm) using a Dektak profilometer. The nominal thickness of ultrathin films can easily be determined by counting arc pulses under the assumption that the deposited film thickness is directly proportional to the number of arc pulses. One needs to stress that film thickness determined this way needs to be understood as nominal, especially at the beginning of the deposition process when the "film" actually consists of islands. The deposition rate was determined to be 0.023 nm/pulse, corresponding to about 1/10 of a monolayer per pulse, an instantaneous rate of 37 nm/s and an average rate of 0.037 nm/s.

For comparison, ultrathin silver films have also been deposited in the same process chamber by dc-magnetron sputtering. The same kinds of substrates were placed 100 mm in front of a 3 in. sputter gun with a silver target. The argon pressure during sputtering was 66 mPa. The sputter power was 40 W with a target potential of -390 V , leading to a deposition rate of 0.75 nm/s.

The essential results are compiled in Fig. 2. The sheet resistance as a function of nominal thickness indicate three

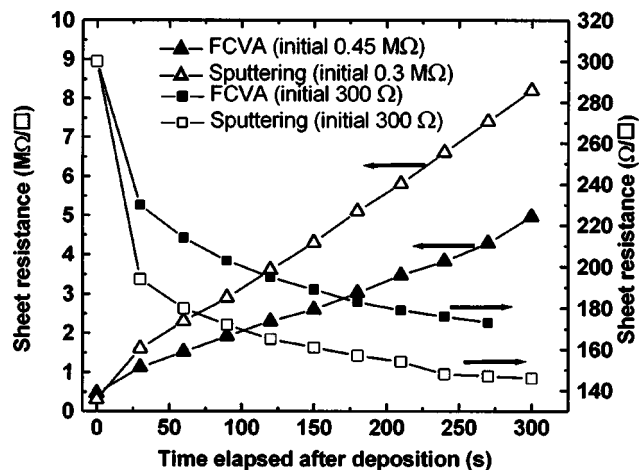


FIG. 3. Sheet resistance of silver films on zinc oxide on glass as a function of time after deposition was stopped.

regions: (i) the region of individually dispersed clusters and islands, (ii) a transition region where short-link conduction starts, and (iii) a region where a continuous film is formed, gradually approaching bulk resistivity when the film thickness exceeds the electron mean free path (Drude model). The energetics of the deposition process and the substrate material and temperature are known to affect the transition region and formation of a continuous film. This is illustrated by the difference between the curves for cathodic arc and magnetron deposited silver on glass and ZnO.

Focusing initially on filtered arc deposition, it was found that silver on oxides exhibit a dynamic behavior. Changes were most pronounced in the transition region shown in Fig. 2. At the beginning of the transition, when the sheet resistance was of order 10 MΩ/□, the continuously monitored sheet resistance increased after the cessation of deposition (Fig 3).

It is known¹¹ that transverse electric current through a growing conducting film can affect film properties. Although the voltage applied here to measure the sheet resistance was only 4.1 V, measurements were repeated several times with the ohm meter either permanently connected or disconnected between measurements in order to identify any transverse current effects if present. It was found that the sheet resistance changed at the same rate regardless of the ohm meter being permanently connected or not.

As successively more silver was deposited on the substrates, the rate of increase in sheet resistance was observed to slow and eventually reverse (Fig. 3). For films with an initial sheet resistance less than a few 10 kΩ/□, the sheet resistance exponentially decreased over time.

Since this dynamic behavior of a not-yet-continuous silver film occurred on a timescale orders of magnitude slower than the atomic deposition process, it can be anticipated that sputtered films show similar behavior. The experiments were repeated with dc magnetron sputtering of silver (Fig. 3).

Pattabi *et al.*¹² showed in an ultrahigh vacuum system that at low surface coverage, the increase in resistance with time is not due to silver oxidation but due to the mobility of silver, leading to the growth of big islands at the expense of smaller islands, thereby minimizing the system energy. This causes the interisland spacing to increase and

the tunneling current between islands to decrease. Our results at low surface coverage can be interpreted with the same argument.

At greater surface coverage, a contiguous film forms between the contact pads, providing short links. Minimization of the system energy can lead to surface diffusion and the thickening of necks between islands that have coalesced. Electronic transport in films at this growth stage can be described by percolation models.¹³ With the exception of a very recent publication on sputtered copper films,¹⁴ aging towards lower sheet resistance has not been reported.

Due to the different energies involved, nucleation and growth processes for evaporation and sputtering differ from processes of energetic deposition. Nucleation and film growth in conventional deposition occurs on the surface of the substrate due to the arrival and motion of film-forming atoms. Nucleation and island formation is governed by adatom mobility, which in turn is determined by the energy of interaction between the surface and the film atoms and the adatom–adatom interaction energy. If the interaction energy between the adatoms and the atoms of the substrate is lower than the energy between the adatoms themselves, the film will grow as discrete islands. Islands grow at the expense of atoms migrating until neighboring islands coalesce, eventually leading to a contiguous and later continuous film.

Nucleation and growth in energetic deposition is different because film-forming ions arrive with high kinetic energy. Cathodic arc Ag ions have an average kinetic energy of 70 eV, as compared to the 1–3 eV in sputter deposition. Dynamic Monte Carlo simulations using the code T-DYN 4.0 indicate that silver ions penetrate TiO₂, for example, with an average range of 1.5 nm, which is several times the mean atomic distance of amorphous TiO₂ (0.22 nm). Subplanted silver changes the actual TiO₂ surface, and therefore it is expected that the film–substrate interface energy be different from the interface energy between pure TiO₂ and Ag.

Temperature is a crucial parameter for film growth. “Temperature” in conventional deposition means the substrate temperature, though the situation is more complicated in energetic condensation. On average, a cathodic arc silver ion delivers 105 eV total energy to the substrate,⁹ which greatly exceeds the lattice and surface binding energies. While the kinetic energy determines the subplantation range, the ion’s potential energy contributes to local heating.⁵ The total energy is released in a nanoscale thermal spike, and diffusion, defect annealing and surface atom migration can occur rapidly. From molecular dynamics simulations it is known that thermal spikes are quenched on a picosecond timescale.

The much slower changes (Fig. 3) indicate that the quenched configurations are thermodynamically not stable. Even at room temperature, the system is driven by thermodynamic forces minimizing the energy stored in the film and its interfaces. For the very thin films considered here, the energy of the free surface and the interfacial energy with the substrate dominate over strain energy and interfacial energies at grain boundaries.¹⁴ Therefore, the type of substrate material is crucial not only for sputtered films but also for films synthesized by energetic condensation. If the interaction en-

ergy between silver and the substrate atoms is high it will reduce the ratio of the maximum height of the island to the island radius, thus reducing the amount of material required to achieve island coalescence. Kinetic energy transfer also facilitates deformation and destruction of existing island structures during energetic deposition. For thicker films, energy minimization by grain growth will occur. Dannenberg *et al.*¹⁰ found activation energies for 80 nm thick silver films to be 0.53 eV for normal and 0.274 eV for abnormal grain growth, indicating that grain growth is dominated by surface diffusion mass transport. The energy of arriving silver ions exceed these threshold energies by more than 2 orders of magnitude and thus one ion can cause motion of many surface atoms.

In summary, the energetic differences between filtered cathodic arc deposition and magnetron sputtering lead to distinct film properties as shown in Fig. 2. Silver films made by cathodic arc deposition show an earlier onset of island coalescence and formation of short links. Silver islands in energetic deposition exhibit a reduced aspect ratio when compared to evaporation and sputtering. However, the as-deposited films are thermodynamically unstable, exhibiting aging on a timescale of minutes. While films of islands tend to increase their sheet resistance with time, contiguous films show a decrease of the sheet resistance. Both effects can be explained by silver mobility driven to minimize film and interfacial energies. Films made by energetic condensation show lower sheet resistance, implying that low-E and solar control layers may have still a margin for improvement.

The authors acknowledge helpful discussions with E. Stach, O. Monteiro, R. Powles, B. Farangis, M. Bilek, D. McKenzie, J. Slack, and M. Rubin. This work was supported by the Laboratory Technology Research Program (SC-32), within the Office of Science, and by the Assistant Secretary for Energy Efficiency and Renewable Energy, Office of Building Technology, U.S. Department of Energy under Contract No. DE-AC03-76SF00098. E.B. was supported by the Post-Doctoral Fellowship Program of the Korean Science and Engineering Foundation (KOSEF).

¹G. B. Smith, G. A. Niklasson, J. S. E. M. Svensson, and C. G. Granqvist, *J. Appl. Phys.* **59**, 571 (1986).

²H. J. Gläser, *Large Area Glass Coating* (Von Ardenne Anlagentechnik, Dresden, Germany, 2000).

³B. Gergen, H. Nienhaus, W. H. Weinberg, and E. M. McFarland, *J. Vac. Sci. Technol. B* **18**, 2401 (2000).

⁴M. Arbab, *Thin Solid Films* **381**, 15 (2001).

⁵A. Anders, *Appl. Phys. Lett.* **80**, 1100 (2002).

⁶A. Bendavid, P. J. Martin, and L. Wiczorek, *Thin Solid Films* **354**, 169 (1999).

⁷R. A. MacGill, M. R. Dickinson, A. Anders, O. R. Monteiro, and I. G. Brown, *Rev. Sci. Instrum.* **69**, 801 (1998).

⁸A. Anders, *Surf. Coat. Technol.* **120–121**, 319 (1999).

⁹A. Anders and G. Y. Yushkov, *J. Appl. Phys.* **91**, 4824 (2002).

¹⁰R. Dannenberg, E. Stach, J. R. Groza, and B. J. Dresser, *Thin Solid Films* **379**, 133 (2000).

¹¹N. Parkansky, B. Alterkop, W. Schuster, R. L. Boxman, and S. Goldsmith, *J. Appl. Phys.* **82**, 4062 (1997).

¹²M. Pattabi, N. Suresh, S. M. Chaudhari, A. Banerjee, D. M. Phase, A. Gupta, and K. M. Rao, *Thin Solid Films* **322**, 340 (1998).

¹³A. I. Maaroof and B. L. Evans, *J. Appl. Phys.* **76**, 1047 (1994).

¹⁴E. V. Barnat, D. Nagakura, P.-I. Wang, and T.-M. Lu, *J. Appl. Phys.* **91**, 1667 (2002).